Parametric Imaging of P-Glycoprotein Function at the Blood–Brain Barrier Using kE,brain-maps Generated from [11C]Metoclopramide PET Data in Rats, Nonhuman Primates and Humans

Louise Breuil, Myriam El Biali, Dominique Vodovar, Solène Marie, Sylvain Auvity, Martin Bauer, Sébastien Goutal, Sebastian Rodrigo, Oliver Langer, Nicolas Tournier

Parametric imaging of P-glycoprotein function at the blood-brain barrier using $k_{E,brain}$-maps generated from [^{11}C]metoclopramide PET data in rats, nonhuman primates and humans

Louise BREUIL[1,2], Myriam ELBIALI[3], Dominique VODOVAR[1,2], Solène MARIE[1], Sylvain AUVITY[1,2], Martin BAUER[3], Sébastien GOUTAL[1], Sebastian RODRIGO[1], Oliver LANGER[3,4], Nicolas TOURNIER[1,*]

1. Inserm, CNRS, CEA, BioMaps, Laboratoire d'Imagerie Biomédicale Multimodale Paris-Saclay, Université Paris-Saclay, Orsay, France.
2. Inserm UMR-S1144, University of Paris Cité, 75006 Paris, France.
3. Department of Clinical Pharmacology, Medical University of Vienna, 1090 Vienna, Austria.
4. Department of Biomedical Imaging and Image-guided Therapy, Medical University of Vienna, 1090 Vienna, Austria.

*** Corresponding author**: Nicolas TOURNIER (PhD., PharmD.)

ORCID:0000-0002-0755-2030

nicolas.tournier@cea.fr

Tel +33.1.69.86.77.12 Fax +33.1.69.86.77.86

CEA/SHFJ, 4 place du Général Leclerc 91400 ORSAY, France

Keywords: ABCB1, ABC transporter, ATP-binding cassette, Pharmacokinetics, Positron Emission Tomography, Multidrug resistance, Neuroimaging

Abstract

Purpose: PET imaging using [^{11}C]metoclopramide revealed the importance of P-glycoprotein (P-gp, ABCB1) in mediating the brain-to-blood efflux of substrates across the blood-brain barrier (BBB). In this work, the elimination rate constant from the brain ($k_{E,brain}$), calculated from dynamic PET images without the need for arterial blood sampling, was evaluated as an outcome parameter for the interpretation of [^{11}C]metoclopramide PET data.

Procedures: $k_{E,brain}$ parameter was obtained by linear regression of log-transformed brain time-activity curves (TACs). $k_{E,brain}$ values (h^{-1}) obtained under baseline conditions were compared with values obtained after complete P-gp inhibition using tariquidar in rats (n=4) and baboons (n=4) or after partial inhibition using cyclosporine A in humans (n=10). In baboons, the sensitivity of $k_{E,brain}$ to measure complete P-gp inhibition was compared with outcome parameters derived from kinetic modeling using a 1-tissue compartment model (1-TCM). Finally, $k_{E,brain}$-maps were generated in each species using PMOD software.

Results: The The linear part of the log-transformed brain TACs occurred from 10-30 min after radiotracer injection in rats, from 15-60 min in baboons and from 20-60 min in humans. P-gp inhibition significantly decreased $k_{E,brain}$ values by 39±12% in rats ($p<0.01$), by 32±6% in baboons ($p<0.001$) and by 37±22% in humans ($p<0.001$). In baboons, P-gp inhibition consistently decreased the brain-to-plasma efflux rate constant k_2 (36±9%, $p<0.01$) leading to an increase in the total brain volume of distribution (V_T, 101±12%, $p<0.001$). In all studied species, brain $k_{E,brain}$-maps displayed decreased P-gp-mediated efflux across the BBB.

Conclusions: $k_{E,brain}$ of [^{11}C]metoclopramide provides a simple outcome parameter to describe P-gp function in the living brain when arterial input function data are unavailable, although less sensitive than V_T. $k_{E,brain}$-maps represent easy to compute parametric images reflecting the effect of P-gp on [^{11}C]metoclopramide elimination from the brain.

Introduction

P-glycoprotein (P-gp, ABCB1) is the most studied efflux transporter expressed at the blood-brain barrier (BBB) [1]. Positron Emission Tomography (PET) imaging using radiolabeled substrates of P-gp provides a unique method to investigate P-gp function in the living brain, in animals and humans [2]. This enabled the validation of pharmacological inhibitors of P-gp function at the BBB, including cyclosporine A and tariquidar [3]. Moreover, PET imaging demonstrated impaired P-gp function at the BBB in several CNS diseases, such as Alzheimer's disease [4, 5].

Outcome parameters to describe P-gp function at the BBB from PET data depend on the pharmacokinetic properties of the investigated probe substrates [6]. The total volume of distribution (V_T), which corresponds to the brain/plasma concentration ratio at steady state, is the gold-standard parameter to describe how P-gp restricts the brain distribution of its substrates [7]. Brain V_T increases as P-gp function decreases, which has been reported for the clinically validated P-gp probes racemic [^{11}C]verapamil [8], (*R*)-[^{11}C]verapamil [9], [^{11}C]*N*-desmethyl-loperamide [10] and [^{11}C]metoclopramide [11].

[^{11}C]Metoclopramide has been specifically designed to detect an induction of P-gp function at the BBB and displays substantial baseline brain uptake when P-gp is normally expressed [12, 13]. [^{11}C]Metoclopramide is specifically transported by the P-gp, not by the Breast Cancer Resistance Protein (BCRP), another efflux transporter at the BBB [13]. Moreover, the BBB penetration of radiolabeled metabolite(s) is negligible, so that the brain PET signal is predominantly composed of parent (unmetabolized) [^{11}C]metoclopramide [13]. This enables the correct estimation of both the plasma-to-brain influx rate constant (K_1) and the brain-to-plasma efflux rate constant (k_2) of parent [^{11}C]metoclopramide using kinetic modeling with a 1-tissue compartment model (1-TCM) (Fig. 1) [14]. This highlighted the prime importance of P-gp-mediated brain-to-plasma efflux (k_2) in limiting [^{11}C]metoclopramide brain exposure [11, 13, 15]. Taking advantage of these properties, the elimination rate constant of [^{11}C]metoclopramide from the brain ($k_{E,brain}$), which can be directly calculated from dynamic PET images without the need of an arterial blood input function (Fig. 1), has been proposed as a parameter to describe P-gp efflux at the BBB in situations of either impaired or induced P-gp function [11, 12, 15].

Parametric maps are useful to represent and visually compare P-gp function in various pathophysiological situations [4, 5]. Parametric maps are also useful for investigating regional changes in P-gp function using voxel-wise statistical mapping. However, the computation of parametric maps describing V_T, K_1 or k_2 requires arterial input function data. In this context, it may be hypothesized that $k_{E,brain}$-maps of [^{11}C]metoclopramide may provide a simplified method to display brain P-gp function at the voxel level. The feasibility and

relevance of [^{11}C]metoclopramide $k_{E,brain}$-maps was evaluated in rats, nonhuman primates and humans.

Material and methods

Data sets

[^{11}C]Metoclopramide PET data used in this analysis, obtained in different species and in different conditions, have been previously reported [11, 15–17]. Data were obtained either in the absence or after P-gp inhibition. Protocols for complete P-gp inhibition could be performed in rats [17] and baboons using tariquidar [15, 18]. Only partial inhibition could be achieved in humans using cyclosporin A (CsA) [11]. Details on image acquisition and data analysis to generate time activity curves (TACs) in the brain are described in the corresponding articles. Experimental conditions used to validate $k_{E,brain}$ are briefly described below.

Ethical approval

All procedures performed in studies involving human participants were in accordance with the ethical standards of the institutional and/or national research committee and with the 1964 Helsinki Declaration and its later amendments or comparable ethical standards. Informed consent was obtained from all individual participants included in the study, as previously described [11]. All applicable institutional and/or national guidelines for the care and use of animals were followed.

PET data in rats

[^{11}C]Metoclopramide PET images were obtained in rats over 30 min in baseline conditions (n=4) and after inhibition of P-gp function with tariquidar (n=4). Tariquidar (8 mg/kg) was i.v. injected 15 min before i.v injection of [^{11}C]metoclopramide [17]. Carbamazepine or ritonavir were used to induce or inhibit cytochrome P450 (CYP) activity, respectively. Carbamazepine suspension (45 mg/kg) was administered orally twice daily for 7 days before the PET imaging (n=4). Animals of the ritonavir group (n=4) received a single oral dose of 20 mg/kg of ritonavir, 3h before [^{11}C]metoclopramide PET imaging [16]. PET data analysis was performed using PMOD software (version 3.9; PMOD Technologies, Zürich, Switzerland). The Schiffer normalization mask was applied to define and isolate the whole-brain and generate time-activity curves (TACs) for this region-of-interest (ROI). Brain radioactivity was corrected for ^{11}C-decay, injected dose and animal weight and expressed as the standardized uptake value (SUV).

PET data in baboons

[^{11}C]Metoclopramide PET data were obtained in 4 different nonhuman primates (baboons) [15]. Each animal underwent [^{11}C]metoclopramide PET imaging at baseline and during P-gp inhibition, achieved by tariquidar infusion (4 mg/kg/h). Tariquidar infusion started at 1 h before radiotracer injection and was continued during the entire PET acquisition (60 min). PET images were generated and reconstructed as previously described. The PET data were analyzed using PMOD software. A baboon MR template was normalized onto individual MR images. PET images were coregistered to this template to delineate and isolate the whole-brain and generate corresponding TACs (SUV *vs* time) [15]. Kinetic modeling was performed using the 1-TCM with the corresponding arterial plasma input function of parent [^{11}C]metoclopramide to estimate the total volume of distribution (V_T; mL.cm^{-3}) as well as the plasma-to-brain influx rate constant (K_1; mL.cm^{-3}.min^{-1}) and the brain-to-plasma efflux rate constant (k_2; min^{-1}, Fig. 1) [15].

PET data in humans

Ten healthy male subjects underwent two consecutive [^{11}C]metoclopramide PET scans without and with P-gp inhibition using CsA infusion (2.5 mg/kg/h), starting 1 h before injection of [^{11}C]metoclopramide and continued for the duration of the PET scan (60 min). Individual T1-weighted MR images were segmented with SPM12 (Statistical Parametric Mapping, Wellcome Trust Centre for Neuroimaging) to define gray and white matter. As previously described, the adult brain maximum probability map ("Hammersmith atlas"; n30r83) was used to extract a whole-brain gray matter ROI [11] and generate TACs (SUV *vs* time) to descrive the brain kinetics of [^{11}C]metoclopramide in this region.

Data and statistical analysis

$k_{E,brain}$ calculation and statistical analysis were performed using GraphPad Prism software (version 9.1.2, GraphPad, La Jolla, CA, USA). $k_{E,brain}$ represents the slope of the linear part of the log-transformed brain TACs and is obtained by linear regression analysis. The time-point of the start of the linear part of the curve (t*) was determined by iterative estimation of $k_{E,brain}$, Earlier time-points were added and linearity was validated until deviation from the previous estimate was >10%. $k_{E,brain}$ was expressed in units of h^{-1} rather than min^{-1} to limit the number of decimals.

The level of statistical significance was set to p<0.05. An unpaired Student's t-test was used to compare the mean values of $k_{E,brain}$ between baseline and P-gp inhibition conditions for rats. The values were considered independent of each other; the normal distribution of the values was verified by the Shapiro-Wilk test and homoscedasticity by an F-test. In addition, a one-way ANOVA with a Dunett's posthoc test was applied to the rat data to compare baseline $k_{E,brain}$ with $k_{E,brain}$ measured in situations of CYP inhibition or induction. Outcome

parameters obtained from the same experiment in the same individual (baboons and humans) were compared using a paired Student's *t*-test. The Shapiro-Wilk test was used to verify the normal distribution of the values.

Construction of $k_{E,brain}$-maps

$k_{E,brain}$-maps were constructed using modules of the PMOD software. First, all images were converted into SUV images in the Pview module. Masks were used to delineate the whole-brain ROI using the isocontour tool in Pview. ROIs were applied to the dynamic coregistered SUV PET images to set the outside voxels to 0 and keep only the dynamic SUV PET image of the whole-brain. These images were opened in the PXMOD module and the regression model was selected. In the input data setting section, the appropriate frames were selected corresponding to the linear part of the TACs, and the logarithm preprocessing tool was applied. In the model calculation tool, the slope pixel-wise calculation was selected and the parametric slope images were built. A scale of –1 multiplication was applied to obtain positive contrast.

Results

Representative TACs for each species are represented in Figure 2. The t* ranged from 5-6 min after radiotracer injection in rats, 7 min for all nonhuman primates, and 10-15 min in humans (data not show). The same time-frame was nonetheless applied to estimate $k_{E,brain}$ in all individuals of the same species: 10-30 min in rats (scan duration: 30 min), 15-60 min in baboons (scan duration: 60 min) and 20-60 min in humans (scan duration: 60 min), which corresponds to linear part of the curve, assessed visually (Fig. 2). In all three species, $k_{E,brain}$ was significantly lower when P-gp was pharmacologically inhibited as compared with the baseline condition ($p<0.01$).

In rats, $k_{E,brain}$ values were similar in carbamazepine-treated and untreated rats ($p>0.05$), whereas ritonavir significantly decreased $k_{E,brain}$ ($p<0.001$, Fig. 3A).

In baboons, $k_{E,brain}$ was 3.3±0.6-fold less sensitive than V_T in terms of response to maximal P-gp inhibition ($p<0.01$) while K_1 and k_2 showed comparable sensitivity to $k_{E,brain}$ (Fig. 3B).

$k_{E,brain}$-maps were generated for each species (Fig. 4). $k_{E,brain}$-maps enabled direct visualization of the impact of P-gp inhibition on efflux transport function (Fig. 4).

Discussion

We here propose a simplified method for quantification and graphical representation of P-gp function at the BBB derived from dynamic [^{11}C]metoclopramide PET data. This quantification method is inspired by the Nuclear Medicine practice to interpret dynamic scintigraphy data obtained with [^{99m}Tc]Tc-sestamibi, another P-gp substrate, to predict tumoral multidrug-

resistance [19]. Compared with brain V_T, which is the gold-standard parameter to measure P-gp function, $k_{E,brain}$ is calculated from dynamic brain PET data only and does not require an arterial input function, which can be challenging to obtain in small animals and patients.

[^{11}C]Metoclopramide shows rapid and substantial initial uptake in the brain, while being rapidly metabolized and cleared from plasma [11, 13, 15]. Therefore, the later part of the brain PET signal, which primarily consists of unmetabolized [^{11}C]metoclopramide, enables reliable calculation of $k_{E,brain}$.

In rats, baboons and humans, $k_{E,brain}$ was shown to display adequate senstivity to measure the impact of pharmacological P-gp inhibition at the BBB. $k_{E,brain}$ was also shown to be sensitive to detect a pharmacological induction of P-gp function at the mouse BBB [12]. The limited impact of CYP induction by carbamazepine on $k_{E,brain}$ suggests that $k_{E,brain}$ may be used as an outcome parameter in patients with drug-resistant epilepsy, who are often treated with CYP-inducing drugs [20]. The significant decrease in $k_{E,brain}$ in ritonavir-treated rats supports previous data suggesting that ritonavir may inhibit P-gp function at the BBB [16]. In baboons, almost maximal inhibition of P-gp could be achieved. Only partial inhibition was achieved in humans, which may explain the lower impact of CsA on $k_{E,brain}$.

There are limitations on the use of $k_{E,}$brain. First, such a quantification method cannot be used for other radiolabeled P-gp substrates which do not benefit from such pharmacokinetic properties. Moreover, $k_{E,brain}$ is less sensitive than V_T to detect maximal P-gp inhibition at the BBB. Maximal change in $k_{E,brain}$ after P-gp inhibition was only similar to the changes in k_2 and K_1, the latter being associated with higher variability. Also, the sensitivity of $k_{E,brain}$ *versus* V_T to detect different level of P-gp function at the BBB remains to be determined. The $k_{E,brain}$ values remained >0 after complete P-gp inhibition in rats and baboons which suggests that $k_{E,brain}$ does not only reflect the P-gp-mediated efflux. Brain-to-blood passive diffusion and peripheral kinetics of [^{11}C]metoclopramide account for $k_{E,brain}$ value. Given substantial differences in the BBB permeation and peripheral clearance of [^{11}C]metoclopramide between rats, nonhuman primates and humans, [11, 13, 15], $k_{E,brain}$ values cannot be used to compared P-gp function across species. Moreover, $k_{E,brain}$ values differ from k_2 values that specifically describe the brain-to-blood transfer constant in the 1-TCM. However, there was a signicant correlation between $k_{E,brain}$ and k_2 values obtained in the same individuals in nonhuman primates (R=0.79, p<0.0001) [15] and humans (R=0.40, p<0.0001) [11].

Finally, we show that $k_{E,brain}$-maps can be easily computed as parametric images to display P-gp-mediated efflux at the BBB. However, calculation of $k_{E,brain}$-maps is associated with some noise and an apparent loss in spatial resolution. $k_{E,brain}$-maps are therefore probably not suited for regional analysis in small animals. However, in baboon or humans, $k_{E,brain}$-maps seem relevant with respect to the brain size and the spatial resolution of clinical PET

scanners. $k_{E,brain}$-maps may be particularly suited to detect focal induction of P-gp at the BBB in epilepsy patients using visual assessment or voxel-wise analysis [20].

Acknowledgments

Funding by ANR19-CE17-0027 (EPIFLUX). LB AND DV received a joined grant from CEA/AP-HP.

Author Contributions,

NT, LB MB and OL designed the study. LB, ME, DV, SM, SA, MB, SG and and SR analyzed the data. LB and NT wrote the first draft of the manuscript. All authors provided critical review and approved the final manuscript.

Conflict of Interest Statement

None

References

1. Abbott NJ, Patabendige AAK, Dolman DEM, et al (2010) Structure and function of the blood-brain barrier. Neurobiol Dis 37:13–25. https://doi.org/10.1016/j.nbd.2009.07.030
2. Kannan P, John C, Zoghbi SS, et al (2009) Imaging the function of P-glycoprotein with radiotracers: pharmacokinetics and in vivo applications. Clin Pharmacol Ther 86:368–377. https://doi.org/10.1038/clpt.2009.138
3. Langer O (2016) Use of PET Imaging to Evaluate Transporter-Mediated Drug-Drug Interactions. J Clin Pharmacol 56 Suppl 7:S143-156. https://doi.org/10.1002/jcph.722
4. Deo AK, Borson S, Link JM, et al (2014) Activity of P-glycoprotein, a β-amyloid Transporter at the Blood-Brain Barrier, is Compromised in Patients with Mild Alzheimer's Disease. J Nucl Med 55:1106–1111. https://doi.org/10.2967/jnumed.113.130161
5. Kortekaas R, Leenders KL, Oostrom JCH van, et al (2005) Blood–brain barrier dysfunction in parkinsonian midbrain in vivo. Annals of Neurology 57:176–179. https://doi.org/10.1002/ana.20369
6. Lubberink M (2016) Kinetic Models for Measuring P-glycoprotein Function at the Blood-Brain Barrier with Positron Emission Tomography. Curr Pharm Des 22:5786–5792. https://doi.org/10.2174/1381612822666160804093852
7. Tournier N, Stieger B, Langer O (2018) Imaging techniques to study drug transporter function in vivo. Pharmacol Ther 189:104–122. https://doi.org/10.1016/j.pharmthera.2018.04.006
8. Muzi M, Mankoff DA, Link JM, et al (2009) Imaging of Cyclosporine Inhibition of P-Glycoprotein Activity Using 11C-Verapamil in the Brain: Studies of Healthy Humans. Journal of Nuclear Medicine 50:1267–1275. https://doi.org/10.2967/jnumed.108.059162
9. Bauer M, Zeitlinger M, Karch R, et al (2012) P-glycoprotein mediated interaction between (R)-[11C]verapamil and tariquidar at the human blood-brain barrier studied with positron emission tomography, a comparison with rat data. Clin Pharmacol Ther 91:227–233. https://doi.org/10.1038/clpt.2011.217
10. Kreisl WC, Liow J-S, Kimura N, et al (2010) P-glycoprotein function at the blood-brain barrier in humans can be quantified with the substrate radiotracer 11C-N-desmethyl-loperamide. J Nucl Med 51:559–566. https://doi.org/10.2967/jnumed.109.070151
11. Tournier N, Bauer M, Pichler V, et al (2019) Impact of P-Glycoprotein Function on the Brain Kinetics of the Weak Substrate 11C-Metoclopramide Assessed with PET Imaging in Humans. J Nucl Med 60:985–991. https://doi.org/10.2967/jnumed.118.219972
12. Zoufal V, Mairinger S, Brackhan M, et al (2020) Imaging P-Glycoprotein Induction at the Blood-Brain Barrier of a β-Amyloidosis Mouse Model with 11C-Metoclopramide PET. J Nucl Med 61:1050–1057. https://doi.org/10.2967/jnumed.119.237198
13. Pottier G, Marie S, Goutal S, et al (2016) Imaging the Impact of the P-Glycoprotein (ABCB1) Function on the Brain Kinetics of Metoclopramide. J Nucl Med 57:309–314. https://doi.org/10.2967/jnumed.115.164350
14. Innis RB, Cunningham VJ, Delforge J, et al (2007) Consensus nomenclature for in vivo imaging of reversibly binding radioligands. J Cereb Blood Flow Metab 27:1533–1539. https://doi.org/10.1038/sj.jcbfm.9600493
15. Auvity S, Caillé F, Marie S, et al (2018) P-Glycoprotein (ABCB1) Inhibits the Influx and Increases the Efflux of 11C-Metoclopramide Across the Blood-Brain Barrier: A PET Study on Nonhuman Primates. J Nucl Med 59:1609–1615. https://doi.org/10.2967/jnumed.118.210104
16. Breuil L, Ziani N, Leterrier S, et al (2022) Impact of Cytochrome Induction or Inhibition on the Plasma and Brain Kinetics of [11C]metoclopramide, a PET Probe for P-Glycoprotein Function at the Blood-Brain Barrier. Pharmaceutics 14:2650. https://doi.org/10.3390/pharmaceutics14122650
17. Breuil L, Marie S, Goutal S, et al (2022) Comparative vulnerability of PET radioligands to partial inhibition of P-glycoprotein at the blood-brain barrier: A criterion of choice? J Cereb Blood Flow Metab 42:175–185. https://doi.org/10.1177/0271678X211045444
18. Bauer M, Karch R, Zeitlinger M, et al (2015) Approaching complete inhibition of P-

glycoprotein at the human blood-brain barrier: an (R)-[11C]verapamil PET study. J Cereb Blood Flow Metab 35:743–746. https://doi.org/10.1038/jcbfm.2015.19
19. Taki J, Sumiya H, Asada N, et al (1998) Assessment of P-glycoprotein in patients with malignant bone and soft-tissue tumors using technetium-99m-MIBI scintigraphy. J Nucl Med 39:1179–1184
20. Feldmann M, Asselin M-C, Liu J, et al (2013) P-glycoprotein expression and function in patients with temporal lobe epilepsy: a case-control study. Lancet Neurol 12:777–785. https://doi.org/10.1016/S1474-4422(13)70109-1

Figures

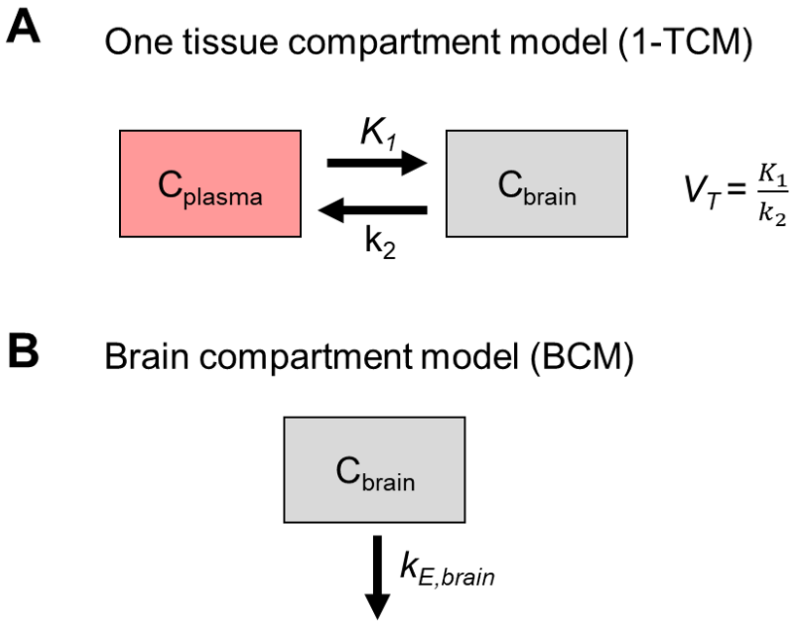

Fig. 1. In A, the one-tissue compartment model (1-TCM), used to describe [^{11}C]metoclopramide distribution across the BBB, is shown. In B, the brain compartment model (BCM) used to determine the elimination rate constant from the brain ($k_{E,brain}$) is shown. C_{plasma} and C_{brain} represent plasma and brain concentraitons of parent [^{11}C]metoclopramide, K_1 is the plasma-to-brain influx rate constant, k_2 is the brain-to-plasma efflux rate constant and V_T is the total volume of distribution.

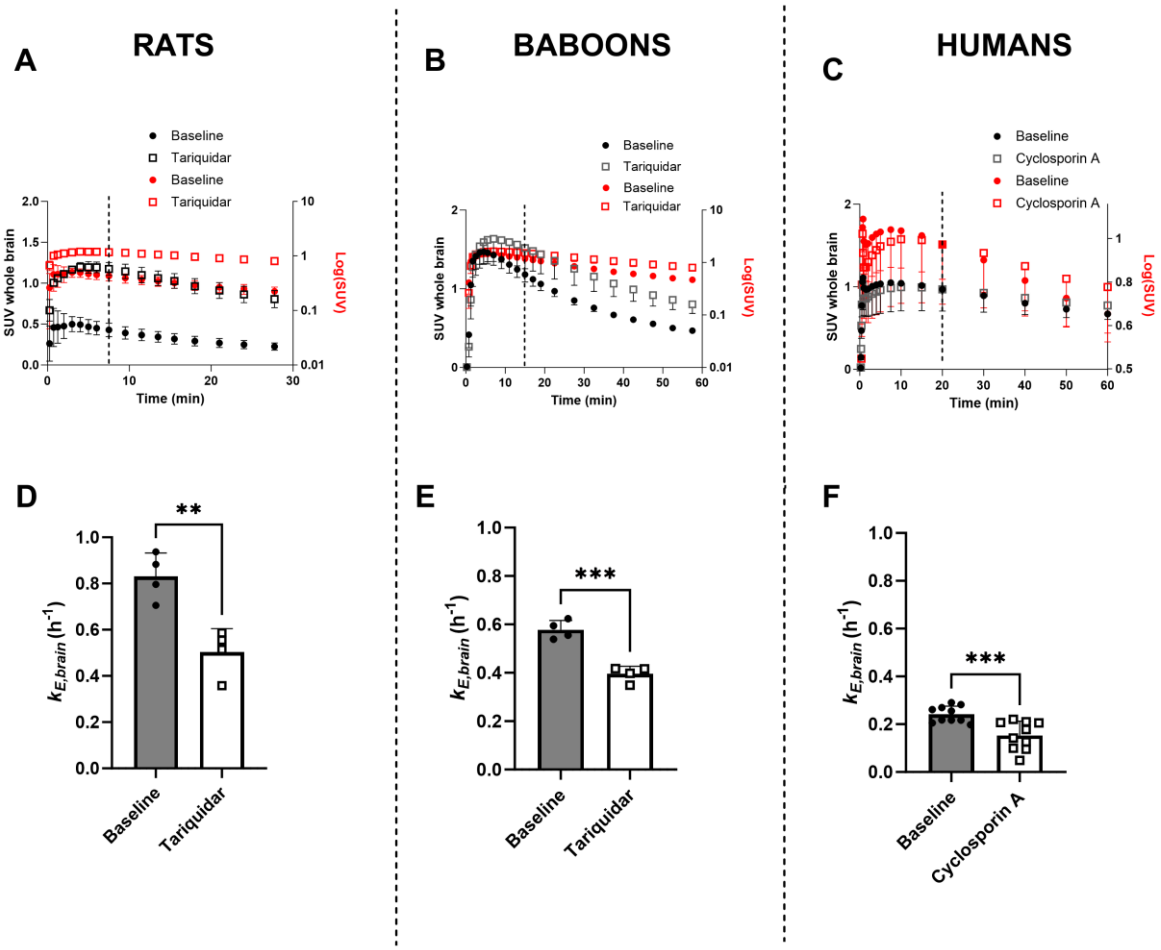

Fig. 2. Mean time-activity curves [^{11}C]metoclopramide in the brain obtained under baseline and P-gp inhibited conditions using either linear (black) or logarithmic (red) scales for rats (A, whole-brain), baboons (B, whole-brain) and humans (C, whole-brain grey matter). $k_{E,brain}$ values obtained under baseline and P-gp inhibited conditions (tariquidar or cyclosporine A) are shown in D for rats (n=4), E for baboons (n=4), and F for humans (n=10). Data are given as mean±SD. ***p<0.001, **p<0.01, unpaired or paired Student's *t*-test

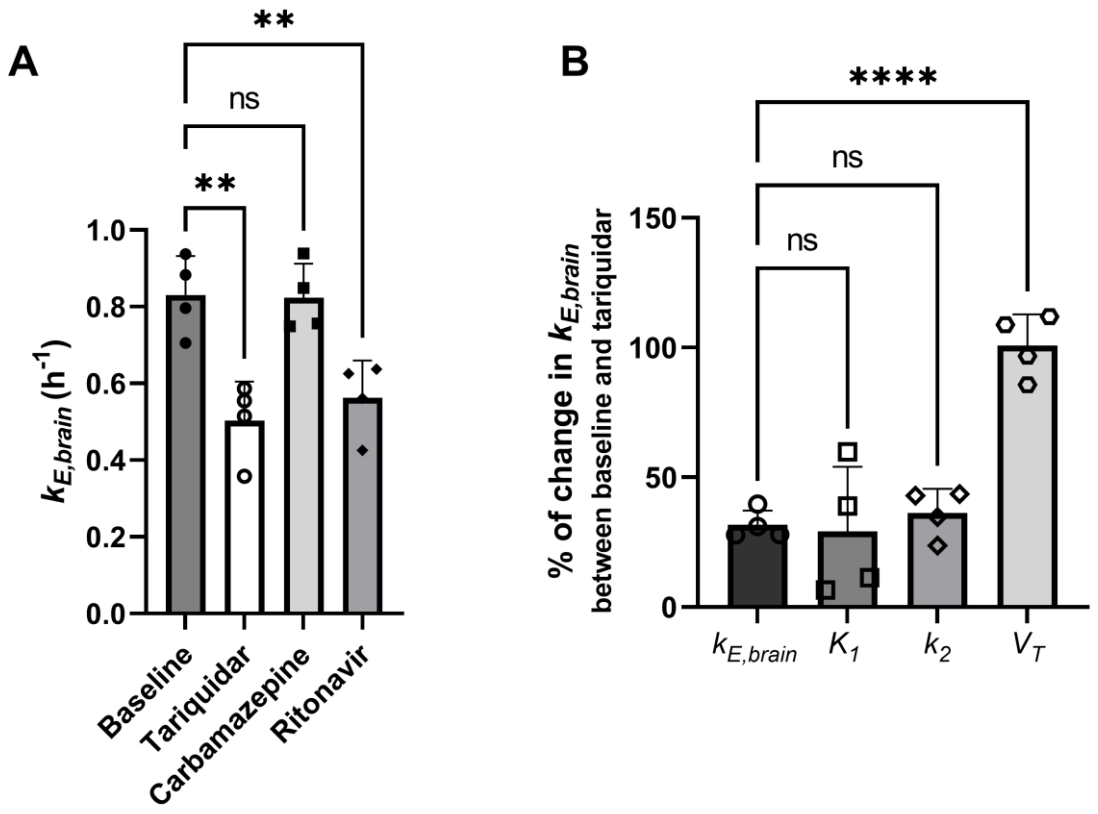

Fig. 3. In A, $k_{E,brain}$ values are shown for untreated (baseline) and tariquidar-, carbamazepine- and ritonavir-treated rat groups. In B, the percentage change of modeling-derived parameters (V_T, K_1, k_2) after P-gp inhibition relative to baseline scans is compared with $k_{E,brain}$ in baboons. ns, not significant, ****p<0.0001, **p<0.01, one-way ANOVA with a Dunett's posthoc test

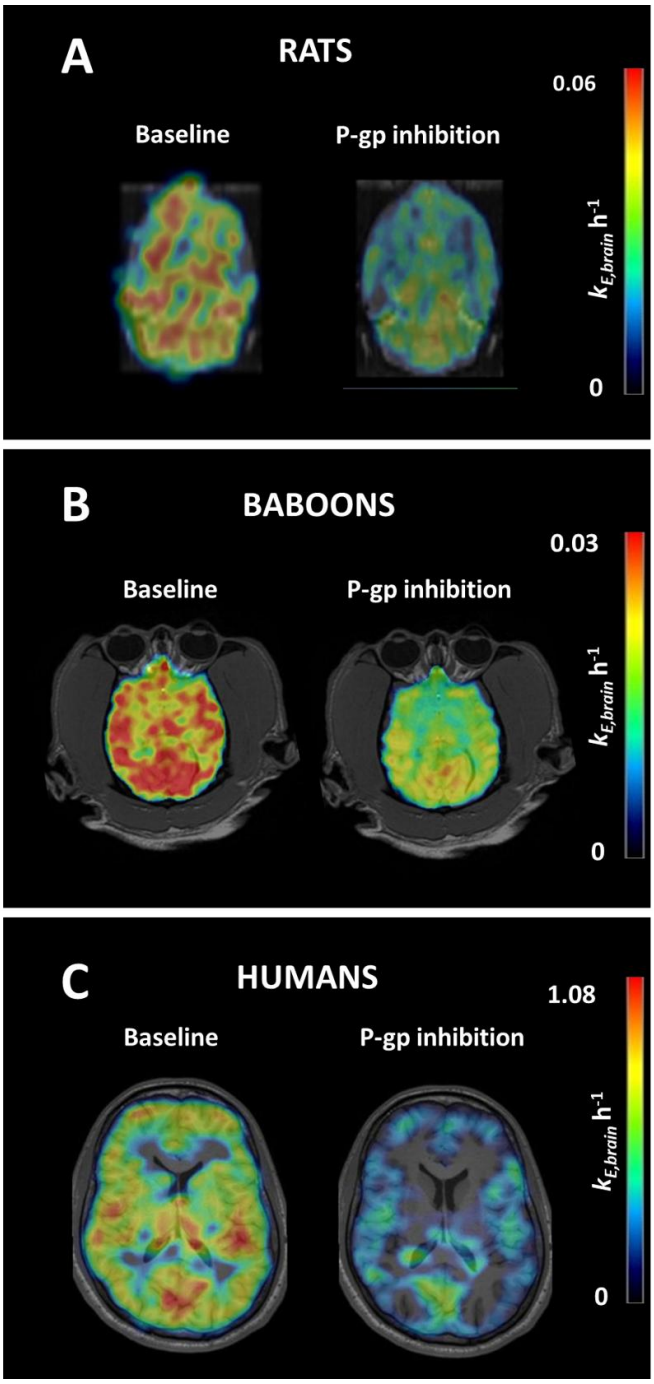

Fig. 4. Representative $K_{E,brain}$-maps under baseline and P-gp inhibited conditions for rats (A), baboons (B), and humans (C).